

A NEW APPROACH FOR MOBIL ROBOT SELF-LOCATION IN THREE DIMENSIONAL ENVIRONMENTS

A. Adán¹, V. Feliu², F. Ramos²

¹*Escuela Superior de Informática.* ²*Escuela Técnica Sup. de Ing. Industriales.*
Universidad de Castilla La Mancha 13071 Ciudad Real (SPAIN)
¹*(aadan@inf-cr.uclm.es),* ²*(vfeliu@ind-cr.uclm.es)*

Abstract: An original mobile robot self-location technique in three dimensional environments is presented in this paper. This method solves the 3D location problem using a single colour camera on board the robot. A very simple pattern consisting of a few color points has been designed in order to achieve two main objectives. pose of the robot in the room and location of the robot in the building. Perspective projection analysis of the pattern is enough to obtain camera viewing parameters in the room coordinate system and color code analysis identifies the specific floor and room in the building. Our approach is being used for applications inside buildings Experimentation with a mobile robot, advantages and restriction of this technique are shown in the paper. *Copyright © 2002 IFAC*

Keywords: Position estimation, Autonomous mobile robots, Computer vision, Robot navigation, Robot vision.

1. INTRODUCTION

Mobile robots must be equipped with several sensors that obtain information from the environment to help the robot determine its location. 3D location implies knowing the coordinates of the robot with respect to specific world coordinate system. For that, sonar, laser, infrared and vision techniques are commonly used. (Neira *et al.* 1999).

In several cases the pose robot problem is solved through camera viewing parameters estimation by processing the information extracted from a single image of a pattern (Tsay, 1987). These approaches are included in monocular perspective projection techniques. Stereo vision techniques have been widely experimented in indoor applications but require higher processing than monocular procedures (Kriegman *et al* 1989). Moreover both cameras must see the whole pattern to carry out image correspondence algorithms. This could be a serious constrain if the mobile robot runs in difficult environments like hospitals or museums where people became an obstacle.

Monocular perspective projection techniques are suitable for on-line autonomous navigation because low processing is required (Guiducci *et al* 2000).

Besides, occlusion problems are easily solved by taking another pattern in the same room.

Different patterns have been designed depending on the environments and accuracy required. Patterns composed of rectangles are used in Haralick (1989), Tsai (1987) and recently in Zhengyou (2000). The corners of the rectangles are the known 3D points and camera parameters are obtained from the corresponding 2D image coordinates of the corners. Kabuba (1987), Adan (1994) and Heikkilä (2000) use projection of circular patterns over a plane to calibrate cameras. A circle of arbitrary radius with two internal dots is used as a pattern for calibration in Han *et al* (1992). All these methods are based on geometric properties of the perspective projection to determine the extrinsic parameters of the camera. Three dimensional patterns are also tested, for example, Chen *et al* (1989) and Marugame *et al* (1999) report the use of a cube.

Most of these methods require precise image preprocessing stages in order to estimate the model from the pattern image. Introduced errors increase if the volume of information to be extracted from the image grows and if the complexity of the features of the objects to be segmented augments. Lens distortion

and digitization process contributes also to increase estimation errors.

When 3D location in indoor environments are considered two aspects must be kept in mind: three dimensional room-coordinates and location in the building. With this purpose, this paper presents a simple pattern with little but enough information encoded on it. The pattern is formed by several sets of color points belonging to concentric circumferences. Maintaining this geometrical structure a color code has been inserted, obtaining a wide and homogenous set of patterns. Our goal is to help the mobile robot determine its absolute location in a building.

The following section describes an overview of our approach: reference model and pattern. Robot self-location in the building, including viewing parameter estimation and room identification procedures, is explained in section 3. Section 4 is devoted to describe the experimental setup and to present the main results. Finally, a summary is stated in the last section.

2. AN OVERVIEW OF THE METHOD.

A projected image of the pattern appears like sets of points belonging to ellipses depending on the viewing position. Perspective projection analysis is enough to obtain the camera viewing parameters: swing (ψ), tilt (ϕ) and pan (θ) angles, and distance D' from the center of the pattern point to the image plane.

Let $(O_w X_w Y_w Z_w)$ be the world coordinate system, and $(O_e X_e Y_e Z_e)$ the camera coordinate system. Camera origin O_e is at the center of the image plane located at the CCD sensor array, and Z_e is in the direction of the optical axis of the camera. Lets assume that camera is always directed to the world origin, which means that optical axis is in the line $O_e O_w$. O_o is the center of the camera optical system, D is the $O_o O_w$ distance, f is focal length ($O_o O_e$ distance) and D' is the $O_e O_w$ distance (see Figure 1).

A pattern is used to help in viewing parameters determination. The pattern has nine points drawn as small color circles over white background. Eight points have identical size and are symmetrically distributed over a circumference of radius R . They appear like the eight vertices of an inner octagon. Each point could be red, green or blue except the point placed on Z_w which is always black. It will be called *first-point* and will be used for identifying the start of the pattern code in the image. Ninth point is bigger than the rest and is located at the center of the octagon. It is called *center-point* (Figure 2 left).

World coordinate system is located at the *center-point* of the pattern. Z_w axis is defined by the *center-point* and the *first-point*. Computer coordinate system $(O_s X_s Y_s Z_s)$ is used to indicate the coordinates of the image in pixels. Finally, the projection of the pattern *center-point* must coincide with the origin O_s in order

to make the optical axis pass through the points O_w and O_e as stated before.

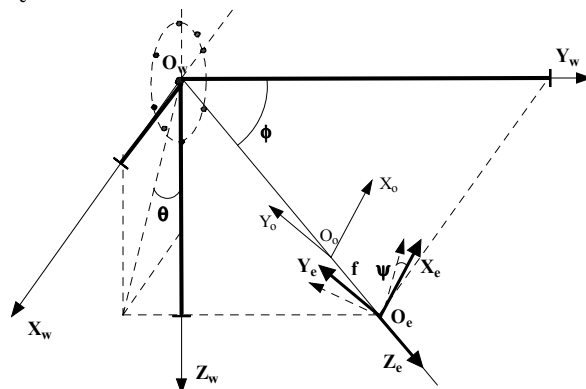


Fig1. Reference model

Swing angle ψ is zero if the ellipse does not appear rotated in the camera coordinate system. Tilt angle ϕ represents the angle formed between the Y_w and Z_e axes. Pan angle θ represents the angle formed between the Z_w and the projection line of the optical axis upon the $Y_w=0$ plane. Finally, the distance from the origin of the camera coordinate O_e system to the origin of the world coordinate system O_w is denoted by D' . As it will show in the next section, pattern image is related to the parameters introduced as follows:

- If $\phi \neq 0$ eight viewed points belong to an ellipse.
- If $\psi \neq 0$ the ellipse seems rotated in the computer reference system.
- If $\theta \neq 0$ *first, third, fifth and seventh points* do not appear over the axes of the ellipse.
- Long axis of the ellipse linearly grows when D' increases.

In order to establish a code, maintaining the same structure of the pattern, we have plotted the points in black (case of *center-point*), red, green or blue colours. This could provide up to 8748 patterns. In section 4, devoted to experimental results, we will present the use of this technique in a building.

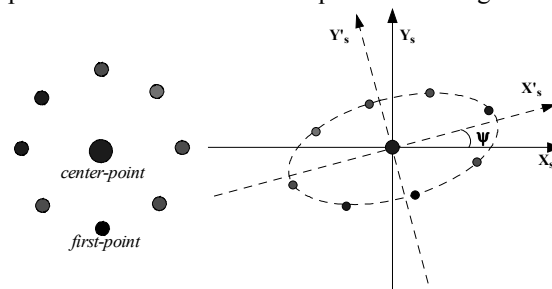


Fig 2. Pattern (left). View of the pattern and ψ angle

3. FULL ROBOT SEFT-LOCATION IN THE BUILDING

In order obtain the full robot location in the building two steps are followed. First, we obtain the 3D pose with respect to a pattern coordinate system and second, we identify the location of the pattern in the building. Next both approaches are presented..

3.1 Obtaining 3D location in the room.

Determination of ψ

This angle coincides in the pattern image with the angle between the long axis of the ellipse and the horizontal reference axis X_s (see Figure 2 right)). A general conic equation must be fitted to the eight points in order to determine this angle. Coefficients A, B, C, D, E and F are the unknowns in this equation. Without loss of generality, F can be fixed to -1. Eight linear equations with five unknowns are obtained from the eight points as follows:

$$A x_i^2 + B x_i y_i + C y_i^2 + D x_i + E y_i = 1 \quad (1)$$

Once this overdetermined system is solved, swing angle ψ can be determined from the estimated parameters A, B and C from equation:

$$\psi = \frac{1}{2} \cdot \arctg \frac{B}{A-C}, \quad A \neq C; \quad \psi = 45^\circ, \quad A = C \quad (2)$$

Determination of the ellipse parameters

To determine the center and the axes of the ellipse a new reference system must be considered. This new system (X'_s, Y'_s) is the original computer reference system rotated an angle ψ .

General conic equation with respect to this system is:

$$A' x'^2 + C' y'^2 + D'x + E'y + F' = 0 \quad (3)$$

where new coefficients are related to the old ones and the angle ψ by:

$$\begin{aligned} A' &= A \cdot \cos^2 \psi + B \cdot \sin \psi \cos \psi + C \cdot \sin^2 \psi \\ B' &= B \cdot \cos 2\psi - (A - C) \cdot \sin 2\psi \\ C' &= A \cdot \sin^2 \psi - B \cdot \sin \psi \cos \psi + C \cdot \cos^2 \psi \\ D' &= D \cdot \cos \psi + E \cdot \sin \psi \\ E' &= E \cdot \cos \psi - D \cdot \sin \psi \\ F' &= F \end{aligned} \quad (4)$$

Assuming that $A' \cdot C' > 0$ and being $A' \neq C'$, the standard ellipse equation is

$$\frac{(x' + D'/2A')^2}{M/A'} + \frac{(y' + E'/2C')^2}{M/C'} = 1; \quad (5)$$

$$M = \frac{D'^2}{4A'} + \frac{E'^2}{4C'} - F'$$

Then, the coordinates of the center, long and short axes of the ellipse with respect to the rotated system and are:

$$x'_c = -\frac{D'}{2A'} \quad y'_c = -\frac{E'}{2C'} \quad a = \sqrt{\frac{M}{A'}} \quad b = \sqrt{\frac{M}{C'}} \quad (6)$$

which are transformed to the computer reference system by means of the expression:

$$\begin{aligned} x_c &= x'_c \cdot \cos \psi - y'_c \cdot \sin \psi \\ y_c &= x'_c \cdot \sin \psi + y'_c \cdot \cos \psi \end{aligned} \quad (7)$$

Determination of ϕ

Figure 3 shows the setup from a view perpendicular to the short axis of the ellipse. Following expressions are derived from this Figure:

$$\frac{b}{x} = \frac{f}{D-y}; \quad \begin{aligned} x &= R \cdot \cos \phi \\ y &= R \cdot \sin \phi \end{aligned} \quad (8)$$

and the next equation is obtained:

$$b = \frac{fR \cdot \cos \phi}{D - R \cdot \sin \phi} \quad (9)$$

Assuming that $R \cdot \sin \phi \ll D$ (which is true in our case) equation (9) converts into:

$$b = \frac{fR}{D} \cdot \cos \phi \quad (10)$$

On the other hand, from a view perpendicular to the long axis of the ellipse, the next relation is found:

$$\frac{a}{R} = \frac{f}{D} \Rightarrow a = \frac{f}{D} R \quad (11)$$

From equations (10) and (11), we obtain

$$\cos \phi = \frac{b}{a} \Rightarrow \sin \phi = e \quad (12)$$

where e is the ellipse eccentricity

Notice that the long axis of the ellipse depends only on the distance from camera to *center-point*, as established in equation (11). Notice also that tilt angle is obtained from eccentricity of the ellipse. Values of ϕ are in the interval $[0, 90^\circ]$, being $\phi=0$ for $e=0$ and $\phi=90^\circ$ for $e=1$.

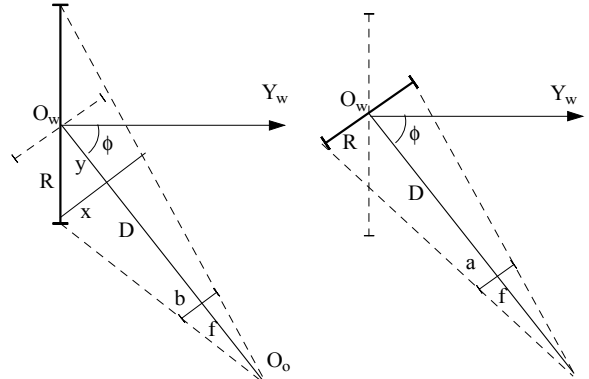


Fig 3. Perpendicular view to the short and the long axis.

Determination of D'

From equation (11) it can be said that distance D from the optical center to the pattern *center-point* is function of only the long axis of the ellipse. Therefore D is independent from the other angular parameters. Given that D' can be measured experimentally we will use D' instead of D as camera viewing parameter.

Next equation defines the focal length f :

$$\frac{1}{f} = \frac{1}{d} + \frac{1}{D} \quad (13)$$

where d represents the distance from the lens's optical center to the image formation plane. Taking into account that $D \gg d$ in the experimental setup, f is a good approximation for d , and equation $D' = D + f$ is verified. It can be used in (11) to estimate D' assuming that f and R are known and a can be obtained from image (a_s in pixels). Because a must be in mm in

equation (11) a proportional factor K_{mm} from a_s to a is required, $a = a_s \cdot K_{mm}$. Where K_{mm} has been determined experimentally from a wide set of images corresponding to different known values of D' . The expression of K_{mm} is the following:

$$K_{mm} = \frac{f \cdot R}{(D' - f) \cdot a_s} \quad (14)$$

Determination of θ .

Let be P a point in the 3D space. Let be $P = P(x_e, y_e, z_e)$ the coordinates of the point with respect to the image plane reference system and $P = P(x_w, y_w, z_w)$ the coordinates of the same point with respect to the world system. Assuming that $\psi = 0$ next homogeneous transformation is verified:

$$(x_e \ y_e \ z_e \ 1) = \begin{pmatrix} \cos \theta & 0 & \sin \theta & 0 \\ \cos \phi \sin \theta & \sin \phi & \cos \phi \cos \theta & 0 \\ \sin \phi \sin \theta & -\cos \phi & \sin \phi \cos \theta & D' \\ 0 & 0 & 0 & 1 \end{pmatrix} \begin{pmatrix} x_w \\ y_w \\ z_w \\ 1 \end{pmatrix} \quad (15)$$

For P being the *first-point* and *fifth-point* whose world coordinates are $(0, 0, R, 1)$ and $(0, 0, -R, 1)$ respectively, the last equation gives:

$$\frac{x_e}{y_e} = \frac{x_s}{y_s} = \frac{\tan \theta}{\cos \phi} \Rightarrow \tan \theta = \frac{x_s}{y_s} \cos \phi \quad (16)$$

For P being the *third-point* and *seventh-point* whose world coordinates are $(R, 0, 0, 1)$ and $(-R, 0, 0, 1)$ respectively, the last equation gives:

$$\frac{x_e}{y_e} = \frac{x_s}{y_s} = \frac{1}{\tan \theta \cos \phi} \Rightarrow \tan \theta = \frac{y_s}{x_s \cos \phi} \quad (17)$$

Then pan angle θ could be obtained from the image coordinates of first, third, fifth and seventh points once angle ϕ was determined. In practice, we have taken the average of them as the final value of θ .

If $\psi \neq 0$, unrotated coordinates x'_s and y'_s must be previously obtained and considered in equations (16) and (17). It can be seen that pan angle estimation depends explicitly on tilt and swing angles estimates. Therefore, errors produced in the estimation of the latest parameters are reflected in the estimation of the former.

3.2 Location of the pattern in the building

In order to identify each pattern we have introduced a colour code in the pattern. Figure 6 c) shows our pattern with a specific code. Distribution of the nine points for coding each information can be easily changed according to the building considered. Information included in the pattern is the following:

- Floor code (f). It identifies the floor where the pattern is. In our case we have chosen *central* (four colours) and *eight point* (three colours) which gives up to 12 floor codes. It is enough for our purpose but more or less points could be taken in the case of buildings with more or less floors.

- Room code (r). It identifies the number of room on each floor. *Second, third, fourth, fifth points* are taken for that. This could code up to 81 rooms/floor.
- Pattern code (p). It identifies the number of pattern in each room. This means that it could have more than one pattern inside every room. For that we have reserved *sixth and seventh points*. So we have the possibility of placing up to 9 patterns/room.

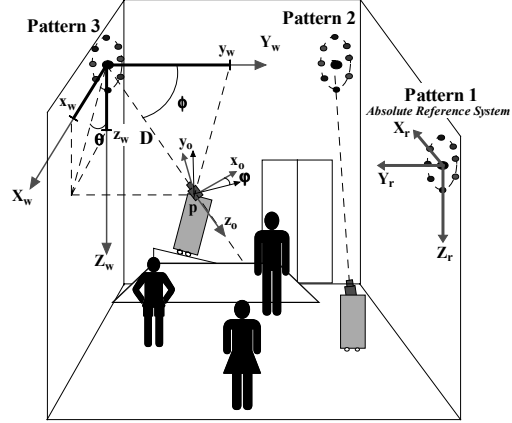


Fig 4. Robot location in a room.

In short, to determine the position of the robot inside the building we could consider six coordinates: (f, r, p, x_w, y_w, z_w) . Where (x_w, y_w, z_w) are coordinates in pattern reference system. As it is clear, transformations between all pattern coordinate systems are known *a priori*. Therefore a building coordinate system (O_b, X_b, Y_b, Z_b) could be defined and (x_b, y_b, z_b) would provide absolute position of the robot. Perhaps this was not a very practical procedure but it could be necessary in any case.

In our case, we have considered an absolute reference system by room (O_r, X_r, Y_r, Z_r) which is fixed on a specific pattern. Then we pass (x_w, y_w, z_w) to (x_r, y_r, z_r) and finally full location of the robot is provided by (f, r, p, x_r, y_r, z_r) . Figure 4 shows a room with several patterns placed on the walls and the absolute reference system chosen.

4. EXPERIMENTAL RESULTS

The proposed method has been tested on multisensor mobile robot QUIXOTE (Fig 5) designed to perform guide tasks in public museums. A controlled azimuth/latitude color camera SONY model EVI D-31, with focal length $f=25\text{mm}$ and autofocus is on board QUIXOTE. Moreover two computers and two frame grabbers accomplish both image processing and camera control.

Color pattern has been designed with two, instead of one, concentric sets of points at 113mm and 72 mm to the *central-point*. We have taken two concentric sets of points (or two pattern) so that the camera could at least be seen one of them completely. On the other hand, Black-R-G-B color coding has been robust enough for our diffuse lighting environment and no other colors has been considered.



Fig 5. QUIXOTE.

The building where we are testing our method has 4 floors with room dimensions of 50m² area and 2,50m high. Patterns have been placed at the top of the wall (2,15m high). Figure 5 right shows patterns placed in a test room. The number of patterns per room depends on the shape and dimensions of each room, but not more than six patterns/room have been used. When the camera looks at a pattern, three parameters are considered for choosing or rejecting it:

- i) Occlusion. The pattern is not completely seen because a person or something is in the way.
- ii) Distance. The pattern is too far and the image of the points is not enough good.

iii) The angle ϕ is too small. In general terms, errors increase for small angles $\phi < 25^\circ$ (low eccentricity), so patterns placed in front of the camera should be rejected. Details of this can be found in Adan, *et al* (1994).

Figure 6 shows the whole process over a image of the pattern. First image processing is performed in order to obtain computer coordinates (x_s, y_s, z_s) (part a)). Noise removal, edge detection and segmentation tasks are accomplished over the original image. Then the label and the color of the points are obtained. Besides an algorithm determines which patters are completely viewed in the image and chooses the bigger as the better pattern. Part b) shows the points, the fitted ellipse and their parameters, ψ, ϕ, θ, D' and the color code of the pattern. In part d) (x_r, y_r, z_r) , their corresponding true values, f, r and p are shown.

Wide experimentation in robot routes is being accomplished with QUIXOTE for museum guide robot purposes. As example Figure 7 shows the results obtained in a path followed by QUIXOTE. 30 pattern images have been taken through the route. Both true and computed paths have been plotted inside the room. As it can be seen in part c) relative errors are quite small. Several images and their corresponding robot locations are marked as well.

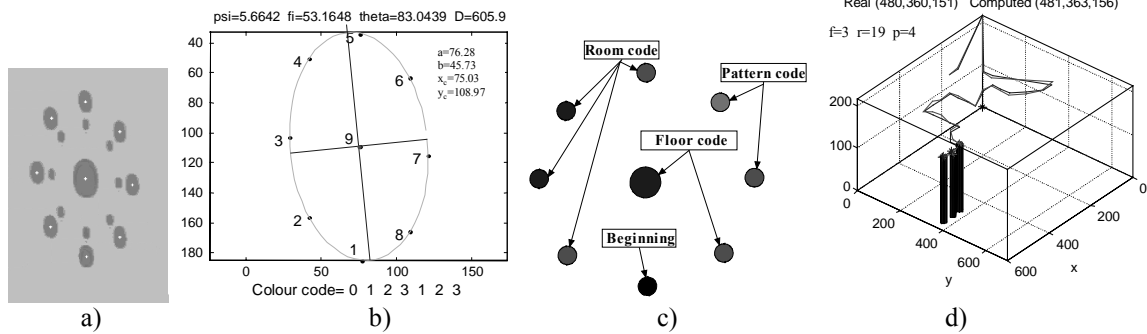


Fig 6. Location process. a) Original image image processing and points location b) fitted ellipse and ellipse parameters c) Pattern code. d) Coordinates and location in the room.

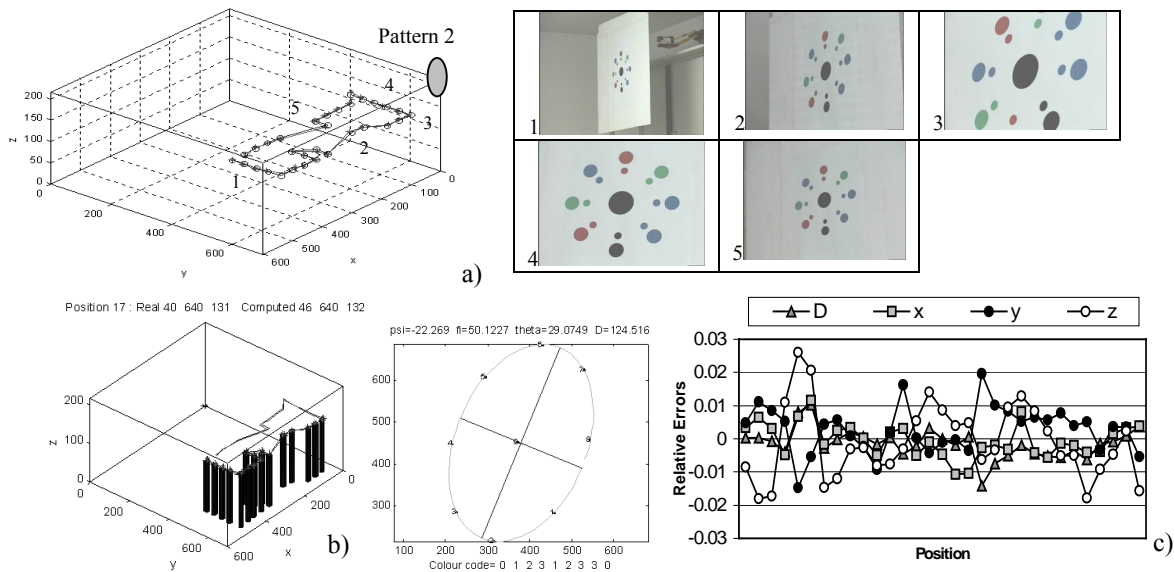


Fig 7.a) Example of a route followed by QUIXOTE, view of the pattern in six positions of the route. b) Detail of position 3 c) Relative errors in the path.

Next a summary of the results is presented. Table 1 summarizes statistical results of the errors obtained for each estimated parameter. Absolute and relative errors are presented in two subtables. For each case, average, standard deviation, greatest and smallest errors are presented as well. Next we will add specific remarks about it.

- Images correspond to distances between 125cm and 800cm from the world origin.
- Average errors are smaller than 0.5% in ϕ estimates and smaller than 1% in θ estimates for all tested images.
- Angle ψ cannot be verified in our setup. Anyway, good results in θ estimations indicate small errors also in ϕ .
- Relative errors in D' estimates are smaller than 0.3% even for small tilt angles.
- Errors in x, y, z are, in the worst case, smaller than 1.3%.
- There were not $f, r,$ and p errors.
- On the other hand, effects due to lens distortion have been ignored because they are very small in our case.

Table 1: Summary of the experimental results.

Abs. Errors	ϕ (°)	θ (°)	D' (cm)	x (cm)	y (cm)	z (cm)
Average.	0.44	0.83	2.89	3.01	2.95	3.09
Std.Dev	0.37	0.84	2.21	2.05	2.43	2.57
Greatest	2.10	3.74	11.30	7.90	11.79	8.16
Smallest	0.05	0.02	0.01	0.06	0.02	0.22
R. Errors (%)	ϕ	θ	D'	x	y	z
Average	0.49	0.92	0.36	0.50	0.49	1.23
Std.Dev	0.40	0.92	0.27	0.34	0.40	1.02
Greatest	2.32	4.01	1.40	1.31	1.96	3.26
Smallest	0.04	0.02	0.001	0.01	0.005	0.09

5. SUMMARY

This method solves the robot 3D location problem using a single colour camera on board the robot. Therefore it is simpler than stereoscopic methods or triangulation based methods where more than one image is used.

3D location involves two things. Firstly, three dimensional room coordinates are computed. This means that the robot is not restricted to run over a flat floor as in 2D navigation. So in 3D navigation, coordinate z could change as well. For instance the robot could go up and down ramps or similar structures. Secondly, a colour code, containing information about location of each room, has been inserted in the pattern. Therefore a full location of a mobile robot can be obtained when the camera looks at a pattern.

Due to the simplicity of the image processing related errors are widely reduced. For instance, segmentation process is performed using elementary thresholding techniques. Next, points are fitted to an ellipse and full location is computed. Both processes are simple and do not introduce significant errors compared to similar approaches. Therefore our method is a fast and robust

method for on-line location. However, it must be mentioned that the method relies on the fact that the optical center, the world origin and the center of the image plane must be in a line. Therefore a technique for target tracking must be performed. When this assumption is not valid, a new source of error is introduced.

Obtained results are good enough to incorporate the proposed method within a research project on mobile robots which is actually being developed in our University. This project is sponsored by CICYT (The Spanish Committee of Science and Technology) and its goal is to use a mobile robot as a museum guide.

REFERENCES

- Adán A. Cerrada C. (1994). Determining camera parameters through the perspective projection of a nine points pattern. *Proc. ISATA'94*. pp279-288.
- Chen Z., Tseng D., Lin J. (1989) A simple vision algorithm for 3-D position determination using a single calibration object. *Pattern Recognition*. **Vol 22**. No 2, pp 173-187.
- Guiducci A. (2000). Camera calibration for Road Applications. *Comp. Vision and Image Understanding*. **Vol 79**, pp 250-266.
- Han M., Rhee S. (1992). Camera calibration for three-dimensional measurement. *Pattern Recognition*. **Vol 25**. No 2, pp 155-164.
- Haralick R.M. (1989). Determining camera parameters from the perspective projection of a rectangle. *Pattern Recognition*. **Vol 22**, No 3, pp 225-230.
- Heikkilä J. (2000). Geometric Camera Calibration Using Circular Control Points. *IEEE Trans PAMI*. **Vol 22**. No 10, pp 1066-1077.
- Kabuka M.R, Arenas A.E. (1987). Position verification of a mobile robot using standard pattern. *IEEE Journal of robotics and automation*. **Vol 3**, No 6.
- Kriegman D. J., Triendl E., Binford T.O. (1989) Stereo vision and navigation in buildings for mobile robots. *IEEE Trans. Robot. Automat.* **Vol 5**, pp 792-803.
- Marugame A., Katto J., Ohta M. (1999). Structure Recovery with Multiple Cameras from Scaled Orthographic and Perspective Views. *IEEE Trans PAMI*. **Vol 21**. No 7, pp 628-633.
- Neira J., Tardós J. Horn J. Schmidt G. (1999). Fusing Range Data and Intensity Images for Mobile Robot Localization. *IEEE Trans. on Robotics and Automation*. **Vol 15**, No 1, pp 76-84.
- Tsai R.Y (1987) A versatile camera calibration technique for high-accuracy 3D machine vision metrology using off-the-shelf TV cameras and lenses. *IEEE Journal of Robotics and Automation*. **Vol 3**, No 4, August 1987.
- Van Albada G.D., Visser A., Lagerberg J.M. and Hertzberger (1995). A low-cost pose measuring system for robot calibration. *Robotics and Autonomous Systems*, **Vol 15**, No 3, pp 207-227.
- Zhang Z. (2000). A Flexible New Technique for Camera Calibration. *IEEE Trans PAMI*. **Vol 22**. No 11, pp 1330-1334.